



Model uncertainties in predictions of arrival of coronal mass ejections at Earth orbit

A. Taktakishvili,^{1,2} P. MacNeice,² and D. Odstrcil³

Received 6 November 2009; revised 3 February 2010; accepted 26 February 2010; published 24 June 2010.

[1] It is very important, both for research and forecasting application, to be aware of uncertainty estimation of a scientific model, i.e., to know how model performance depends on the uncertainty in the input parameters. Scientific models are becoming more important as tools for space weather operators' applications and for space weather forecasting. It is essential that operational users, forecasters, model developers, and the scientific community are aware of model capabilities and limitations. In our previous study we validated the performance of the WSA/ENLIL cone model combination in simulating the propagation of 14 events of coronal mass ejections (CMEs) to the L1 point using the cone model approach for halo CMEs. In this short report we present the results of the uncertainty estimation for the WSA/ENLIL cone model combination studying the dependence of the arrival time of the CME shock and the magnitude of the CME impact on the magnetosphere on the uncertainty in the CME input parameters using three events from the previously reported 14 event list.

Citation: Taktakishvili, A., P. MacNeice, and D. Odstrcil (2010), Model uncertainties in predictions of arrival of coronal mass ejections at Earth orbit, *Space Weather*, 8, S06007, doi:10.1029/2009SW000543.

1. Introduction

[2] The advantage of scientific modeling is that it provides a global view of a studied phenomenon, something that is not available using only satellite or ground observations. Scientific models are becoming more and more important as tools for understanding and forecasting the physical processes in the solar system. Models are used for space weather operators' applications and for space weather forecasting. It is essential that the operational users, forecasters, model developers and the scientific community are aware of model capabilities and limitations. Since modeling results depend on the input parameters, it is very important, both for forecasting applications and research, to estimate the robustness of the model performance dependence on the uncertainty in the input parameters. In this paper we present the results of such uncertainty estimation for the WSA/ENLIL cone model in predictions of arrival of coronal mass ejections (CMEs) at Earth orbit.

[3] In our previous work [Taktakishvili *et al.*, 2009] we studied the performance of the WSA/ENLIL cone model in modeling the propagation of CMEs in the heliosphere. A CME is an ejection of material from the solar corona, that can be detected remotely with a white light corona-

graph. When the CME reaches the Earth as an interplanetary CME (ICME), it may disrupt the Earth's magnetosphere, compressing it on the dayside and extending the nightside tail. The most severe geomagnetic storms are caused by ICME events [Gosling, 1993]. ICMEs can result in damage to satellites, disruption of radio transmissions, damage to electrical power transformers and power outages. That is why knowing accurate arrival times of ICMEs at the Earth is of crucial importance in predicting space weather. There have been extensive observational as well as theoretical studies of CMEs in relation to their space weather implications in the recent decade. We briefly reviewed most of them in the work by Taktakishvili *et al.* [2009], so here we present only the references [Berdichevsky *et al.*, 2000; Gopalswamy *et al.*, 2001, 2005; Kim *et al.*, 2007; Fry *et al.*, 2003; Oler, 2004; Dryer *et al.*, 2004; Smith *et al.*, 2005; McKenna-Lawlor *et al.*, 2006; Wu *et al.*, 2007; Tóth *et al.*, 2007; Lugaz *et al.*, 2007].

[4] The WSA/ENLIL cone model has two components, (1) cone model for halo CMEs, an analytical method to determine the angular width, propagation direction and radial velocity of halo CMEs, developed by Xie *et al.* [2004], and (2) the ENLIL heliosphere model, a time-dependent 3-D MHD model of the heliosphere, developed by D. Odstrcil [see, e.g., Odstrcil and Pizzo, 1999; Odstrcil *et al.*, 2004]. In the work by Taktakishvili *et al.* [2009] we reported the results of the ENLIL cone model for 14 CME events and compared them to ACE observations. We focused on two parameters, the arrival time of the CME shock and the magnitude of the CME impact on the magnetosphere. The

¹Goddard Earth Science and Technology Center, University of Maryland, Baltimore County, Baltimore, Maryland, USA.

²NASA Goddard Space Flight Center, Greenbelt, Maryland, USA.

³Department of Computational and Data Sciences, George Mason University, Fairfax, Virginia, USA.

magnitude of the CME impact is characterized by the magnetospheric magnetic field magnitude needed to stop the CME mass flow. The corresponding magnetopause standoff distance was also calculated. We used version 2.5 of the ENLIL model available currently at the Community Coordinated Modeling Center at NASA/GSFC.

[5] In this paper we perform uncertainty estimation of the WSA/ENLIL cone model, studying the dependence of the arrival time of the CME shock and the magnitude of the CME impact on the magnetosphere on the uncertainty in the CME input parameters using 3 events from the previously reported 14 event list.

2. Brief Description of the Cone Model, the WSA/ENLIL Models, and the Objective of the Uncertainty Estimation

[6] Zhao *et al.* [2002] were the first to propose the cone model approximation to determine CME geometric and kinematic parameters using an iterative method for CME image analysis. They assumed that a CME propagates with nearly constant angular width in a radial direction and that the expansion is isotropic. Based on this idea, Xie *et al.* [2004] developed an analytical method for determining parameters of halo CME, angular width of the cone, propagation direction and radial speed, directly from coronagraph images. We used the method developed by Xie *et al.* [2004] in our previous paper [Taktakishvili *et al.*, 2009] determining CME cone model parameters from LASCO C3 coronagraph images. These parameters are used as input to the ENLIL heliosphere model to study the CME propagation out to the ACE location at the L1 point. The method of Xie *et al.* [2004] is based on a geometrical analysis of a CME white light image contour and the assumption that this contour has an “elliptical” shape which is considered to be a projection of a CME cone on the plane of the sky. Naturally this is a rather simplistic approximation of a CME and the result depends on the “ellipse” contour determination. Our experience with deriving CME parameters from LASCO C3 images [Taktakishvili *et al.*, 2009] showed that the cone orientation is rather robust, while velocity is rather sensitive to the ellipse contour determination.

[7] In this paper we used three previously studied events, to investigate how the uncertainty in velocity determination manifests itself in the WSA/ENLIL cone model results with regard to the CME shock arrival time and also the magnitude of the CME impact on the magnetosphere. We also explore how the uncertainty in cone opening angle influences the model results.

[8] ENLIL is a time-dependent 3-D MHD model of the heliosphere [Odstrcil and Pizzo, 1999]. It solves equations for plasma mass, momentum and energy density, and magnetic field, using a Total-Variation-Diminishing Lax-Friedrichs algorithm. Its inner radial boundary is located beyond the sonic point (where the solar wind flow becomes supersonic), typically at 21.5 solar radii. ENLIL can accept boundary condition information from the

empirical Wang-Sheeley-Argge (WSA) coronal model [Arge and Pizzo, 2000]. WSA models the global magnetic field between the solar surface and a bounding spherical surface, where the magnetic field is assumed to be radial. The photospheric magnetic field is determined from synoptic magnetogram data. WSA computes the solar wind speed at the bounding surface using an empirical relationship. ENLIL applies this WSA output at its inner boundary and propagates the solar wind, including the CME, throughout the heliosphere.

[9] In ENLIL, the CME as an initially spherical plasma cloud, has a uniform velocity. The temperature is assumed to be the same as in the ambient fast solar wind. There is a free parameter of the ratio of the CME cloud density to the ambient fast solar wind density, which cannot be derived from the observations. We call it density factor “df.” In our previously reported study [Taktakishvili *et al.*, 2009], df was equal to 4 by default. Thus, the plasma cloud had about four times larger pressure than the ambient fast wind. The CME cone model is based on observational evidence that a CME has more or less constant angular diameter in the corona, being confined by the external magnetic field, so that the CME does not expand in latitude in the lower corona, but expands later in interplanetary space due to the weaker external field. This is naturally a simplification, but launching of an overpressured plasma cloud at $21.5R_{\odot}$, roughly represents development of a coronal mass ejection expanding into the interplanetary space [see, e.g., Odstrcil *et al.*, 2004].

[10] In the presented work we performed the uncertainty estimation of the WSA/ENLIL cone model results due to uncertainty in initial velocity, cone angular radius, and density factor. We chose three CME events from the previous solar cycle: (1) “high-speed” CME event of 13 December 2006; (2) “moderate-speed” CME event of 6 April 2001; and (3) “low-speed” CME event of 15 April 2002. Varying each of the parameters by the factor of approximately 2, we studied the influence of this variation on the CME transit time (CME arrival time to the L1 point) and the magnitude of the CME impact on the magnetosphere.

[11] In the simulations presented here, ENLIL in most of the cases uses relatively low resolution spatial grid $256 \times 30 \times 90$, where 256 is the number of equally spread grid points in the radial direction (range from 0.1 AU to 2 AU), 30 is the number of equally spread grid points in the latitude (perpendicular to the equatorial plane, range from -60° to $+60^\circ$), and 90 is the number of equally spread grid points in the longitude (range from 0° to 360°). The spatial resolution used is rather coarse. This has the benefit of using less computing time and resources. Run execution time length for these parameters is approximately 2 h on a 4 processor machine, which is much faster than real time and is a very good characteristic for forecasting purposes. In order to study the impact of the different spatial resolution on the model sensitivity to initial conditions we also performed two additional runs for one of the studied events

(13 December 2006 CME) with higher resolution in radial direction, using grids $512 \times 30 \times 90$ and $1024 \times 30 \times 90$.

3. Uncertainty Estimation for the CME Shock Arrival Time

[12] The 13 December 2006, sometimes called the “AGU storm” CME, was the last significant halo CME in the previous solar cycle. This is considered as a high-speed event in the presented work. The observed transit time of the CME shock was 35 h. In the SOHO/LASCO catalog (http://cdaw.gsfc.nasa.gov/CME_list/) the CME plane of sky projection velocity at $20 R_s$ is listed as $V_{POS} \sim 1573$ km/s. Our estimation of the radial velocity from the LASCO C3 images using cone model method of Xie *et al.* [2004] yielded $V \sim 2170$ km/s [Taktakishvili *et al.*, 2009]. The estimation of the cone half angular width (CME cone opening half-angle) gave 67° for this case. Assuming that the density factor $df = 4$, we use these values as base parameters for this high-speed event.

[13] For the 6 April 2001 event, the SOHO/LASCO catalog lists the CME plane of sky projection velocity at $20 R_s$ as $V_{POS} \sim 1215$ km/s (http://cdaw.gsfc.nasa.gov/CME_list/). For the radial velocity from the LASCO C3 images using the cone model method we obtained $V \sim 1570$ km/s [Taktakishvili *et al.*, 2009]. This is the considered as a moderate-speed event in our analysis. The observed transit time of the CME shock was 39 h. The estimated cone half angular width for this event is 79° . With the density factor $df = 4$, we use these values as base parameters for this moderate-speed event.

[14] The 15 April 2002 CME event is considered as a low-speed event in our study. The observed transit time of the CME shock was 52 h. The SOHO/LASCO catalog lists the CME plane of sky projection velocity at $20 R_s$ as $V_{POS} \sim 731$ km/s. The estimated radial velocity and cone half angular width are correspondingly $V \sim 736$ km/s and 74° . With $df = 4$, we use these values as base parameters for this low-speed event.

[15] In the work by Taktakishvili *et al.* [2009] we compared the CME shock arrival times predicted by the WSA/ENLIL cone model simulations to the observed (ACE) shock arrival times for 14 studied events. The prediction error,

$$\Delta t_{err} = t_{enlil}^{arr} - t_{obs}^{arr} \quad (1)$$

is negative when the model predicted a shock arrival time earlier than the observed shock arrival time, and is positive for late ENLIL prediction. For the 13 December 2006 CME the model shock arrival time error was ~ -5 h; that is, the model predicted the CME shock arrival ~ 5 h earlier than actual arrival [Taktakishvili *et al.*, 2009]. The observed shock transition time, time interval between the first appearance of the CME in LASCO C2 coronagraph image and the CME shock arrival observed by the ACE satellite, was ~ 35 h. For the 6 April 2001 and 15 April 2002 events, the model shock arrival time error (observed shock

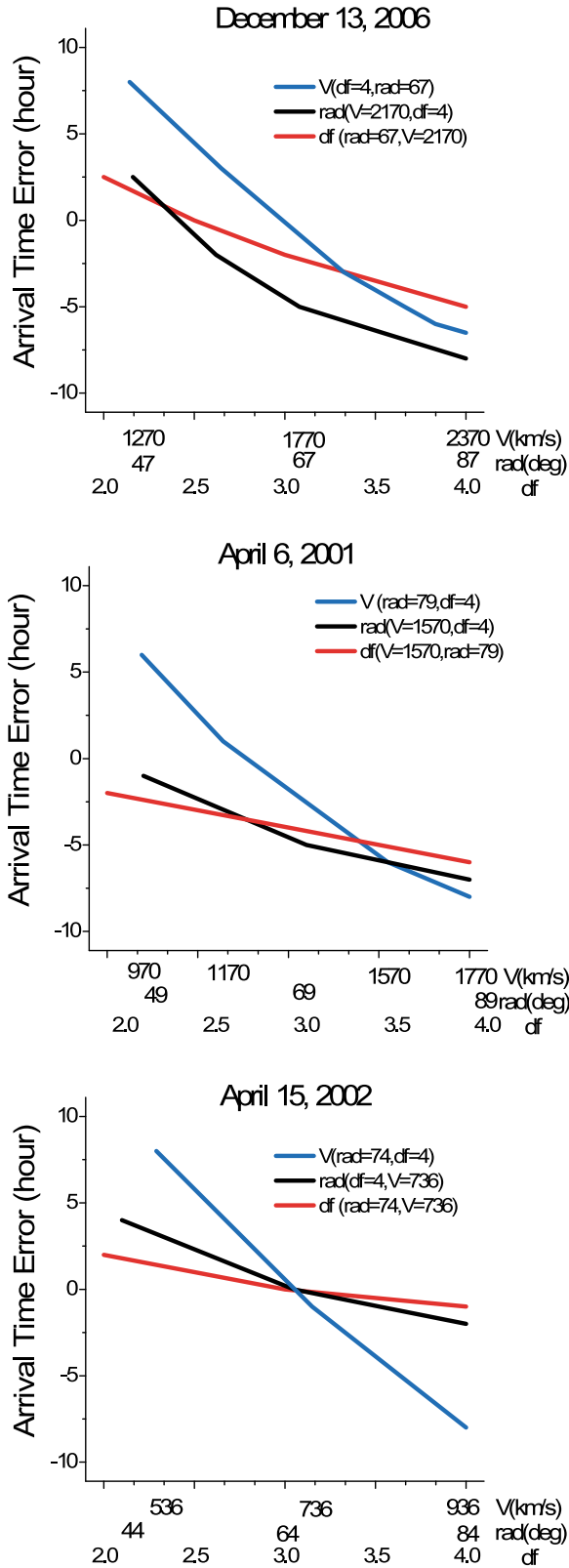
transition time) was ~ -6 h (~ 39 h) and ~ -1 h (~ 52 h), correspondingly.

[16] It is important to know the dependence of arrival time error on the uncertainty in the input parameters. We performed the uncertainty estimation of the shock arrival time with respect to three input parameters: (1) initial radial velocity, derived from the cone model using LASCO C3 images; (2) cone half angular width, half of the opening angle of the CME cone; and (3) density factor, a parameter equal to the ratio of the CME material density to the ambient fast solar wind density, which cannot be derived from the observations presently.

[17] Figure 1 displays the shock arrival time error dependence on the input initial parameters for all three events.

[18] Figure 1 (top) shows the results for high-speed 13 December 2006 event, where we used the values: 1270, 1570, 1970, 2270, 2370 km/s for V ; 47° , 57° , 67° , 77° , 87° for the cone half angular width; and 2, 2.5, 3, 3.5, 4 for the density factor. So, almost 2 fold (or exactly 2 fold, in case of the density factor) variation of each of the input parameters. The blue line represents the dependence of the arrival time error on radial velocity of the CME, V , for $df = 4$ and cone half angular width equals 67° . As you can see almost 2 fold variation of the input velocity results in the variation of the arrival time error from about -6.5 h to about 8 h. This shows that the shock arrival time error is not very robust relative to uncertainty in the input velocity. If we interpolate between the velocity stamps, the shock arrival time error would be zero for $V \sim 1800$ km/s. The black line shows the arrival time dependence on the input cone half angular width, which varies from 47° to 87° , for $V = 2170$ and $df = 4$. The arrival time error varies in this case from about -8 h to about 2.5 h; that is, the window of arrival time uncertainty due to the uncertainty in cone half angular width is more narrow than due to the uncertainty in the velocity. We can conclude for the CME transit time the model is more robust with respect to the uncertainty due to the cone input geometry than due to the uncertainty in the input velocity, which is a reasonable result. Finally, the red line presents the shock arrival time error dependence on the uncertainty in the density factor, which varies from $df = 2$ to $df = 4$, for $V = 2170$ and cone half angular width 67° . Figure 1 (top) clearly shows more robustness of the model result for the shock arrival time than in two previous cases. The window of uncertainty extends from about -5 h to about 2.5 h. Thus, for the CME shock arrival time for the 13 December 2006 CME, the largest window of uncertainty of the model, due to the approximately two fold uncertainty in the input parameters, is $[-8, 8]$ h. The percentage of the largest uncertainty window width relative to the observed propagation time (let us call it “relative uncertainty”) is about 46%.

[19] Figure 1 (middle) displays the shock arrival time error dependence on the input initial parameters for the moderate-speed 6 April 2001 event, where we used the values: 970, 1170, 1370, 1570, 1770 km/s for V ; 49° , 59° , 69° ,



79°, 89° for the cone half angular width; and 2, 2.5, 3, 3.5, 4 for the density factor. The color coding is the same as in Figure 1 (top). Almost 2 fold variation of the input velocity for $df = 4$ and cone half angular width equals 79°, results in the variation of the arrival time error from about -8 h to about 6 h. So, the dependence of the arrival time error on the uncertainty in the input velocity for this moderate-speed event is close to the previous case of high-speed 13 December 2006 CME. The arrival time error due to uncertainty in the cone half angular width, for $V = 1570$ and $df = 4$, varies from about -7 h to about -1 h; that is, the dependence is slightly weaker than in the previous case of high-speed CME. The shock arrival time error variation due to the uncertainty in the density factor for fixed velocity $V = 1570$ and cone half angular width equals 79, is the smallest in comparison to the variation due to the uncertainties in velocity and cone half angular width. This result is similar to the previous case of high-speed 13 December 2006 CME event. The dependence of the arrival time error on the uncertainty in the density factor is weaker than it is for high-speed CME event of 13 December 2006. The window of uncertainty extends from about -6 h to about -2 h. The largest window of uncertainty of the model for this moderate-speed event, due to the approximately two fold uncertainty in the input parameters, is [-8, 6] h. The relative uncertainty in this case is about 36%.

[20] Finally, Figure 1 (bottom) displays the shock arrival time error dependence on the input initial parameters for the low-speed 15 April 2002 CME event, where we used the values: 536, 636, 736, 836, 936 km/s for V ; 44°, 54°, 64°, 74°, 84° for the cone half angular width; and 2, 2.5, 3, 3.5, 4 for the density factor. The color coding is the same as in

Figure 1. The shock arrival time error dependence on the initial input CME radial speed, CME cone half angular width, and CME to ambient solar wind density ratio (density factor). (top) High-speed, 13 December 2006 CME event. The blue line represents the variation due to the variation of the input radial velocity, V , for $df = 4$ and cone half angular width equals 67°. The black line shows the dependence on the input cone half angular width, for $V = 2170$ and $df = 4$. The red line represents the shock arrival time error dependence on the uncertainty in the density factor for $V = 2170$ and cone half angular width 67°. (middle) Moderate-speed, 6 April 2001 CME event. Color coding is the same as in Figure 1 (top): blue line for $df = 4$ and cone half angular width equals 79°, black line for $V = 1134$ and $df = 4$, and red line for $V = 1134$ and cone half angular width 79°. (bottom) Low-speed, 15 April 2002 CME event. Color coding is the same as in Figure 1 (top and middle): blue line for $df = 4$ and cone half angular width = 74°, black line for $V = 736$ and $df = 4$, and red line for $V = 736$ and cone half angular width 74°.

Figure 1 (top and bottom). Almost 2 fold variation of the input velocity for $df = 4$ and cone half angular width equals 74° , results in the variation of the arrival time error from about -8 h to about 8 h, the result close to the previous cases of high- and moderate-speed CMEs. The arrival time error due to uncertainty in the cone half angular width, for $V = 736$ and $df = 4$, varies from about -2 h to about 4 h; that is, the dependence is weaker than in the previous cases of high- and moderate-speed CMEs. So, the dependence on the cone half angular width becomes weaker for lower-speed CMEs. Finally, the shock arrival time error variation due to the uncertainty in the density factor for fixed velocity $V = 736$ and cone half angular width equals 74 , shows the weakest dependence, in comparison to uncertainty in velocity and cone half angular width. This is similar to the previous cases of high- and moderate-speed CMEs. For the low-speed CME of 15 April 2002 this dependence is weaker than in the case of moderate-speed CMEs. The window of uncertainty extends from about -1 h to about 2 h. So, similar to the dependence on the cone half angular width, the dependence on the density factor becomes weaker for lower-speed CMEs. Interestingly enough all curves in Figure 1 (bottom) meet approximately in one point corresponding to the almost zero arrival time error, for $V \sim 700$ km/s, cone half angular width ~ 60 and $df = 3$. So this is the “ideal” combination of the parameters for the ENLIL cone model for this particular event. The largest window of uncertainty of the model for this low-speed CME event, due to the approximately two fold uncertainty in the input parameters, is $[-8, 8]$ h. The relative uncertainty in this case is about 31%.

[21] Summarizing this section we can conclude that, for the predicted CME shock arrival error, (1) the dependence on the uncertainty in the CME speed is the strongest out of dependencies on the three discussed parameters; it is similar to all three, high-, moderate- and low-speed, CME events; (2) the dependence on the uncertainty in the CME cone half angular width is the second strongest and becomes weaker for lower-speed CMEs; and (3) the dependence on the uncertainty in the density factor is the weakest and similar to the dependence on the cone half angular width, it becomes weaker for lower-speed CMEs.

[22] The largest window of uncertainty of the arrival time, due to the approximately two fold uncertainty in the input parameters, is $[-8, 8]$ h regardless CME speed. The relative uncertainty for high-, moderate- and low-speed events is correspondingly 46%, 36%, and 31%.

4. Uncertainty Estimation for the Magnitude of Impact and Resulting Magnetopause Standoff Distance

[23] Another parameter important for the space weather forecasters and operators is the magnitude of the impact of the CME on the magnetosphere. We measure this parameter by the degree of the deformation of the Earth's magnetosphere due to the interaction with the CME. In

the work by *Taktakishvili et al.* [2009] we assumed that the physical quantity mostly responsible for the strength of the impact of the CME on the magnetosphere is a dynamic pressure of the solar wind. The magnetic field that would be required to “stop” the solar wind stream was estimated from the equation given by *Spreiter et al.* [1965]:

$$Knm_pV^2 = \frac{B_{stop}^2}{2\mu_0} \quad (2)$$

where K is a constant that characterizes the degree of reflection of the solar wind stream from the current sheath boundary, n and V are the solar wind number density and plasma velocity, respectively, m_p is the proton mass and B_{stop} is the corresponding magnetosphere magnetic field. In ideal case of completely “elastic” reflection $K = 2$, and $K = 1$ for “inelastic” reflection. In the case of high Mach number solar wind, $K \simeq 0.881$ [*Spreiter et al.*, 1965], and we will use this value for K in our analysis.

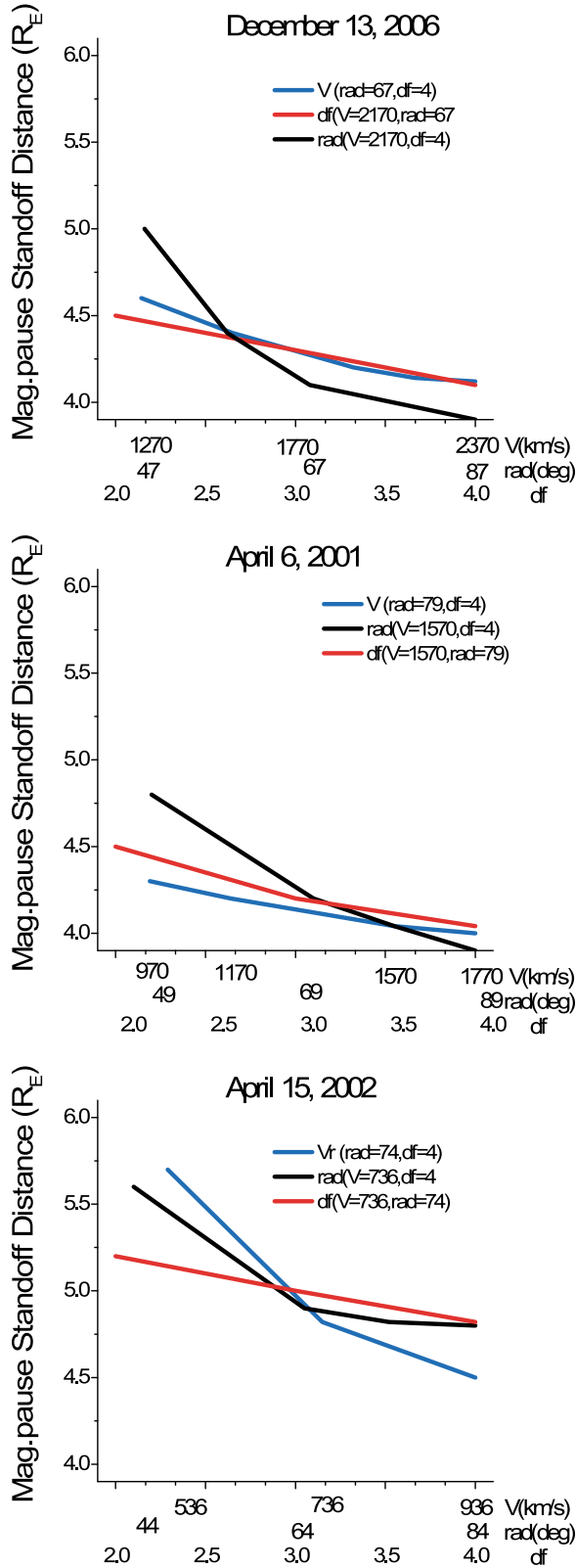
[24] This equation yields the following expression for the magnetic field:

$$B_{stop} = V\sqrt{1.762nm_p\mu_0} \quad (3)$$

[25] Now we can characterize the anticipated response of the Earth's magnetosphere to the CME impact in another way. If we assume that the magnetic field close to the Earth is a dipole, $B = B_0(R_E/r)^3$, where $B_0 = 3.11 \cdot 10^4$ nT and R_E is the Earth's radius, then inserting $B = B_{stop}$ into this equation will give an approximate expression for the magnetopause standoff distance:

$$r = \left(\frac{B_0}{B_{stop}}\right)^{1/3} R_E \quad (4)$$

[26] Figure 3 (bottom) of *Taktakishvili et al.* [2009] displays the evolution of the standoff distance for the 13 December 2006 CME event estimated by the WSA/ENLIL cone model. The WSA/ENLIL cone model overestimated the ram pressure impact for all 14 events reported by *Taktakishvili et al.* [2009] as it is clear from their Figure 4. The model pushes the magnetopause closer to the Earth than would be expected from the ACE measurements of the solar wind ram pressure. The minimum magnetopause standoff distance for the 13 December 2006 CME event, derived from the ACE observations, yields $r_{min} \sim 5.6R_E$, while the model estimate is $\sim 4.1R_E$, which is a pretty significant difference. But, note that the lower limit of the estimated standoff distance corresponds to the instantaneous peaks of the ICME disturbance at the magnetopause and that these value probably will not be sustained for a long period of time. The current ENLIL version assumes a spherical homogeneous cloud launched in the heliosphere which gives a large momentum (dynamic pressure). The discrepancy should be smaller in



the upcoming version of ENLIL with the flux-rope-like structure.

[27] Although the model strongly overestimates the CME impact on the magnetosphere, it is still important to estimate how the predicted magnetopause standoff distance depends on the uncertainty in the input parameters. We performed the uncertainty estimation for the same input parameters and the same conditions as in section 3.

[28] Figure 2 (top) shows the minimum magnetopause standoff distance for the high-speed 13 December 2006 CME event. The color coding is the same as in Figure 1. The dependence on the velocity V for $df = 4$ and cone half angular width equals 67° is shown in blue. The standoff distance varies from $\sim 4.1R_E$ to $\sim 4.6R_E$. This shows that the magnetopause standoff distance does not depend strongly on the uncertainty in the input velocity for this high-speed CME event. The standoff distance dependence on the input cone half angular width for $V_r = 2170$ and $df = 4$ is shown in black. The standoff distance varies from $\sim 3.9R_E$ to $\sim 5R_E$; that is, the window of uncertainty due to the uncertainty in cone half angular width is more than 2 times wider than due to the uncertainty in the speed. This strong dependence on the cone half angular width is obviously due to the quadratic dependence of the total mass content in the CME on the cone half angular width. Finally, the red line clearly demonstrates that the standoff distance depends the least on the uncertainty in the density factor: for $V = 2170$ km/s and cone half angular width equals 67° , the window of uncertainty extends from $\sim 4.1R_E$ to $\sim 4.5R_E$ in this case. The largest window of uncertainty of the model due to the almost 2 fold uncertainty in the parameters for the high-speed CME event is $[3.9R_E, 5R_E]$.

[29] Figure 2 (middle) shows the minimum magnetopause standoff distance for the moderate-speed 6 April 2001 CME event. The minimum magnetopause standoff distance for this event, derived from the ACE observations, yields $r_{\min} \sim 6.12R_E$. The blue line demonstrates the weak dependence of standoff distance variation (from $\sim 4R_E$ to $\sim 4.3R_E$), due to the almost 2 fold variation of the input velocity for $df = 4$ and radius equals 79° . The standoff distance depending on the input cone half angular width for $V = 1570$ and $df = 4$, shown in black, varies from $\sim 3.9R_E$ to $\sim 4.8R_E$; that is, the window of uncertainty due to the uncertainty in cone half angular width is more than 2.5 times wider than due to the uncertainty in the velocity. The red line in Figure 2

Figure 2. The minimum magnetopause standoff distance dependence on the initial input CME radial speed, CME cone half angular width, and CME to ambient solar wind density ratio (density factor). (top) High-speed, 13 December 2006 CME event. (middle) Moderate-speed, 6 April 2001 CME event. (bottom) Low-speed, 15 April 2002 CME event. Color coding is the same as in Figure 1.

Table 1. Arrival Time and Magnetopause Standoff Distance for Different Spatial Resolutions for the High-Speed 13 December 2006 CME

	Resolution		
	Low	Medium	High
CME shock arrival time on 14 Dec 2006 (UT)	0910	0748	0718
Magnetopause standoff distance (R_E)	4.13	4.1	4.0

(middle) demonstrates that the window of uncertainty due to uncertainty in the density factor, for $V = 1570$ km/s and cone half angular width equals 79° , extends from $\sim 4R_E$ to $\sim 4.5R_E$, i.e., a bit less than in the case of high-speed CME. This shows also that for moderate-speed CME the magnetopause standoff distance dependence on the uncertainty in the density factor is slightly stronger than dependence on the uncertainty in the speed. The largest window of uncertainty of the model due to the almost 2 fold uncertainty in the parameters for this case of moderate-speed CME is $[3.9R_E, 4.8R_E]$.

[30] Figure 2 (bottom) shows the minimum magnetopause standoff distance for the low-speed 15 April 2002 CME event. The standoff distance varies from $\sim 4.5R_E$ to $\sim 5.7R_E$ for almost 2 fold variation of the input velocity and fixed $df = 4$, radius equals 74° . So, the magnetopause standoff distance strongly depends on the uncertainty in the input velocity in this case of low-speed CME. The dependence on the input cone half angular width for $V = 736$ and $df = 4$ shown in black, demonstrates the variation of the standoff distance from $\sim 4.8R_E$ to $\sim 5.6R_E$. So, unlike the previous cases, the window of uncertainty due to the uncertainty in cone half angular width is more narrow than due to the uncertainty in the velocity. The red line in Figure 2 (bottom) demonstrates that the standoff distance depends the least on the uncertainty in the density factor for fixed $V = 736$ km/s and cone half angular width equals 74° . The window of uncertainty extends from $\sim 4.8R_E$ to $\sim 5.2R_E$. Thus, for the magnetopause standoff distance, the largest window of uncertainty of the model due to the almost 2 fold uncertainty in the parameters for this case of low-speed CME is $[4.5R_E, 5.7R_E]$.

[31] From the discussion in this section we can conclude that, for the predicted magnetopause standoff distance, (1) the dependence on the uncertainty in the CME initial speed is weak for high- and moderate-speed CME events and relatively strong for low-speed CMEs; (2) the dependence on the uncertainty in the CME cone half angular width is the strongest for high- and moderate-speed CMEs and relatively strong, but weaker than dependence on the uncertainty in the initial speed, for low-speed CME; and (3) the dependence on the uncertainty in the density factor is the weakest for high- and low-speed CME events and slightly stronger than the dependence on the uncertainty in initial speed for moderate-speed CME.

[32] The largest window of uncertainty in the magnetopause standoff distance, due to the approximately two fold uncertainty in the input parameters, is $[3.9R_E, 5.7R_E]$.

5. Impact of the Resolution on the Model Results

[33] In this section we present a brief study of the impact of the resolution on the model results.

[34] Table 1 shows the arrival time and magnetopause standoff distance predicted by the model for different spatial resolutions in radial direction. In this example we used the high-speed 13 December 2006 CME with base parameters: initial radial speed 2170 km/s, CME cone opening half-angle 67° , and the density factor 4. The low resolution corresponds to the grid $256 \times 30 \times 90$, medium resolution corresponds to the grid $512 \times 30 \times 90$, and high resolution corresponds to the grid $1024 \times 30 \times 90$.

[35] The actual shock arrival for this event was around 1400 UT on 14 December 2006. The magnetopause standoff distance corresponding to ACE data is $\sim 5.63 R_E$. As we can see from the Table 1 the arrival time predicted by the model shifts by 1 h 22 min toward earlier prediction during the transition from low to medium resolution, thus making the arrival time error bigger. Clearly the reason for this is more fine shock front structure in case of medium resolution. The further two fold increase of the resolution shifts the CME shock arrival time 30 min further toward earlier prediction, indicating that the shock front resolution is becoming saturated.

[36] Therefore, in case of earlier than observed shock arrival prediction, the increase of the resolution leads to increase of the arrival time error. One can expect that in the opposite case of later than observed arrival prediction, the increase of the resolution will lead to improvement of the prediction result. So, this demonstrates that the shock arrival time may vary substantially according to different spatial resolutions used. On the contrary, the magnetopause standoff distance almost does not depend on the resolution, as it is clear from the Table 1.

[37] The influence of the resolution on the model results is an important issue and needs more thorough analysis, which is beyond the scope of this paper. This can be subject of a separate publication.

6. Summary

[38] It is very important, both for research and forecasting application, to be aware of uncertainty estimation of a scientific model, i.e., to know how the model performance depends on the uncertainty in the input parameters.

[39] We performed the uncertainty estimation for the WSA/ENLIL cone model combination. We studied the dependence of the predicted CME shock arrival time error on the uncertainty in the CME input parameters. We focused on three parameters in this paper: (1) initial radial speed of a CME, (2) CME cone half angular width, and (3) CME material to ambient solar wind density ratio. We also studied the dependence of the predicted magnitude of the

CME impact on the magnetosphere, manifested in the magnetopause standoff distance, on the uncertainty in the same parameters.

[40] We analyzed three events from the previously reported *Taktakishvili et al.* [2009] 14 event list: (1) relatively high initial speed, 13 December 2006 CME; (2) moderate-speed, 6 April 2001 CME; and (3) relatively low initial speed, 15 April 2002 CME.

[41] For the uncertainty estimation of the CME arrival time error we can conclude the following.

[42] 1. The dependence of the arrival time error on the uncertainty in the CME speed is the strongest of the dependencies on the three discussed parameters. It is similar in high-, moderate- and low-speed CME events.

[43] 2. The dependence on the uncertainty in the CME cone half angular width is the second strongest. It is weaker for lower-speed CMEs.

[44] 3. The dependence on the uncertainty in the density factor is the weakest. Similar to the dependence on the cone half angular width, it is weaker for lower-speed CMEs.

[45] The dependence of the magnetopause standoff distance on the three parameters is more complicated and varies for different initial speed CMEs: (1) the dependence on the uncertainty in the CME initial speed is weak for high- and moderate-speed CME events and relatively strong for low-speed CMEs; (2) the dependence on the uncertainty in the CME cone half angular width is the strongest for high- and moderate-speed CMEs and relatively strong, but weaker than dependence on the uncertainty in the initial speed, for low-speed CME; and (3) dependence on the uncertainty in the density factor is the weakest for high- and low-speed CME events and weak but slightly stronger than the dependence on the uncertainty in initial speed for moderate-speed CME.

[46] The overall conclusion of these studies is, that in most of the cases, uncertainty in the CME initial speed and CME cone half angular width are the most important parameters for CME shock arrival time and magnetopause standoff distance, respectively, while the uncertainty in CME density has the least influence on the model prediction. The window of uncertainty due to the approximately two fold uncertainty in the input parameters was [−8, 8] h for the arrival time regardless of the CME initial speed. This yielded arrival time window widths relative to observed transit times of no more than 46%. For the magnetopause standoff distance, the window of uncertainty is almost $2R_E$.

[47] We also found that the shock arrival time may vary as a function of the model spatial resolutions used, while the magnetopause standoff distance is largely independent of resolution.

[48] Finally, we acknowledge that the information gathered from this study is only an initial investigation. Eventually, for the WSA/ENLIL cone model to become a fully validated operational predictor of CMEs, a more comprehensive study, based on hundreds or even thousands of simulations, where controls are changed

both independently and in conjunction of each other, will be needed.

[49] **Acknowledgments.** D.O. was partially supported by NSF/CISM and NASA/LWS grants. All simulations carried out in this work were done at the Community Coordinated Modeling Center at NASA Goddard Flight Center.

References

- Arge, C. N., and V. J. Pizzo (2000), Improvement in the prediction of solar wind conditions using near-real time solar magnetic field updates, *J. Geophys. Res.*, **105**, 10,465–10,479.
- Berdichevsky, D. B., A. Szabo, R. P. Lepping, and A. F. Vinas (2000), Interplanetary fast shocks and associated drivers observed through the 23rd solar minimum by Wind over its first 2.5 years, *J. Geophys. Res.*, **105**, 27,289–27,314.
- Dryer, M., Z. Smith, C. D. Fry, W. Sun, C. S. Deehr, and S.-I. Akasofu (2004), Real-time shock arrival predictions during the “Halloween 2003 epoch,” *Space Weather*, **2**, S09001, doi:10.1029/2004SW000087.
- Fry, C. D., M. Dryer, Z. Smith, W. Sun, C. S. Deehr, and S.-I. Akasofu (2003), Forecasting solar wind structures and shock arrival times using an ensemble of models, *J. Geophys. Res.*, **108**(A2), 1070, doi:10.1029/2002JA009474.
- Gopalswamy, N., A. Lara, S. Yashiro, M. Kaiser, and R. Howard (2001), Predicting the 1-AU arrival times of coronal mass ejections, *J. Geophys. Res.*, **106**, 29,207–29,217.
- Gopalswamy, N., A. Lara, P. K. Manoharan, and R. Howard (2005), An empirical model to predict the 1-AU arrival of interplanetary shocks, *Adv. Space Res.*, **36**, 2289–2294.
- Gosling, J. T. (1993), The solar flare myth, *J. Geophys. Res.*, **98**, 18,937–18,949.
- Kim, K.-H., Y.-J. Moon, and K.-S. Cho (2007), Prediction of the 1-AU arrival times of CME-associated interplanetary shocks: Evaluation of an empirical interplanetary shock propagation model, *J. Geophys. Res.*, **112**, A05104, doi:10.1029/2006JA011904.
- Lugaz, N., W. B. Manchester IV, I. I. Rouseev, G. Toth, and T. I. Gombosi (2007), Numerical investigation of the homologous coronal mass ejection events from active region 9236, *Astrophys. J.*, **659**, 788–800.
- McKenna-Lawlor, S. M. P., M. Dryer, M. D. Kartalev, Z. Smith, C. D. Fry, W. Sun, C. S. Deehr, K. Kecskemety, and K. Kudela (2006), Near real-time predictions of the arrival at Earth of flare-related shocks during Solar Cycle 23, *J. Geophys. Res.*, **111**, A11103, doi:10.1029/2005JA011162.
- Odstrcil, D., and V. J. Pizzo (1999), Distortion of the interplanetary magnetic field by three-dimensional propagation of coronal mass ejections in a structured solar wind, *J. Geophys. Res.*, **104**, 28,225–28,240, doi:10.1029/1999JA900319.
- Odstrcil, D., P. Riley, and X. P. Zhao (2004), Numerical simulation of the 12 May 1997 interplanetary CME event, *J. Geophys. Res.*, **109**, A02116, doi:10.1029/2003JA010135.
- Oler, C. (2004), Prediction performance of space weather forecast centers following the extreme events of October and November 2003, *Space Weather*, **2**, S08001, doi:10.1029/2004SW000076.
- Smith, Z., T. R. Detman, M. Dryer, and C. D. Fry (2005), Determining shock velocity inputs for Sun-to-Earth models, in “Connecting Sun and Heliosphere”: *Proceedings of Solar Wind 11/SOHO 16*, edited by B. Fleck and T. H. Zurbuchen, *Eur. Space Agency Spec. Publ.*, ESA SP592, 771–774.
- Spreiter, J. R., A. L. Summers, and A. Y. Alksne (1965), Hydromagnetic flow around the magnetosphere, *Planet. Space Sci.*, **14**, 223–253.
- Taktakishvili, A., M. Kuznetsova, P. MacNeice, M. Hesse, L. Rastätter, A. Pulkkinen, A. Chulaki, and D. Odstrcil (2009), Validation of the coronal mass ejection predictions at the Earth orbit estimated by ENLIL heliosphere cone model, *Space Weather*, **7**, S030004, doi:10.1029/2008SW000448.
- Tóth, G., D. L. De Zeeuw, T. I. Gombosi, W. B. Manchester, A. J. Ridley, I. V. Sokolov, and I. I. Rouseev (2007), Sun-to-thermosphere simulation of the 28–30 October 2003 storm with the Space Weather Modeling Framework, *Space Weather*, **5**, S06003, doi:10.1029/2006SW000272.

- Wu, C.-C., C. D. Fry, S. T. Wu, M. Dryer, and K. Liou (2007), Three-dimensional global simulation of interplanetary coronal mass ejection propagation from the Sun to the heliosphere: Solar event of 12 May 1997, *J. Geophys. Res.*, *112*, A09104, doi:10.1029/2006JA012211.
- Xie, H., L. Ofman, and G. Lawrence (2004), Cone model for halo CMEs: Application to space weather forecasting, *J. Geophys. Res.*, *109*, A03109, doi:10.1029/2003JA010226.
- Zhao, X. P., S. P. Plunkett, and W. Liu (2002), Determination of geometrical and kinematical properties of halo coronal mass ejections using the cone model, *J. Geophys. Res.*, *107*(A8), 1223, doi:10.1029/2001JA009143.
-
- P. MacNeice and A. Taktakishvili, NASA Goddard Space Flight Center, Greenbelt, MD 20771, USA. (aleksandre.taktakishvili-1@nasa.gov)
- D. Odstrcil, Department of Computational and Data Sciences, George Mason University, Fairfax, VA 22030, USA.